Ali, I., Barrett, B., Cawkwell, F., Green, S., Dwyer, E. and Neumann, M. (2017) Application of repeat-pass TerraSAR-X staring spotlight interferometric coherence to monitor pasture biophysical parameters: limitations and sensitivity analysis. *IEEE Journal of Selected Topics in Applied Earth Observations and Remote Sensing*, 10(7), pp. 3225-3231. (doi:10.1109/JSTARS.2017.2679761)

Sensitivity Analysis of Repeat-Pass TerraSAR-X Staring Spotlight InSAR Coherence To Monitor Pasture Biophysical Parameters (Height, Biomass)

Iftikhar Ali, Brian Barrett, Fiona Cawkwell, Stuart Green, Edward Dwyer, and Maxim Neumann, *Member, IEEE*

***Abstract*—This paper describes the potential and limitations of repeat-pass synthetic aperture radar interferometry (InSAR) to retrieve the biophysical parameters of intensively managed pastures. We used a time series of 8 acquisitions from the TerraSAR-X Staring Spotlight (TSX-ST) mode. The ST mode is different from conventional Stripmap mode therefore we adjusted the Doppler phase correction for interferometric processing. We analysed the three interferometric pairs with an 11-day temporal baseline, and among these three pairs found only one gives a high coherence. The results show that the high coherence in different paddocks is due to cutting of the grass in the month of June, however the temporal decorrelation in other paddocks is mainly due to the grass growth and high sensitivity of the X-band SAR signals to the vegetation cover. The InSAR coherence (over coherent paddocks) shows a good correlation with SAR backscatter ($R^2_{dB} = 0.65,\ p < 0.05$) and grassland biophysical parameters ($R^2_{Height} = 0.55,\ p < 0.05$, $R^2_{Biomass} = 0.75,\ p < 0.05$). It is thus possible to detect different management practices (e.g., grazing, mowing/cutting) using SAR backscatter (dB) and coherence information from high spatial, short baseline X-band imagery, however the rate of decorrelation over vegetated areas is high.**

***Index Terms*—Biophysical parameters, TerraSAR–X Staring Spotlight, interferometry, managed pastures, InSAR coherence.**

I. Introduction

GRASSLANDS are one of the most prevalent and widespread land cover vegetation types, covering 31.5% of the global landmass [1]. After forests, grasslands are the largest terrestrial carbon sink [2] and, as such, play a vital role in regulating the global carbon cycle. Most of the earth observation studies on grasslands have been based on optical imagery for various applications e.g., classification, biomass, conservation status and growth rate [3], [4]. But in recent years, after the launch of high-resolution spaceborne SAR sensors like TerraSAR-X (X-band German SAR sensor launched in 2007) and COSMO-SkyMed (X-band constellation of four Italian satellites launched in 2007 to 2010), new investigations on grasslands using SAR data regarding mapping [5], monitoring management strategies [6] and parameter retrievals [7] have been reported in the research literature.

The literature suggests that, with the development and availability of spaceborne SAR data with improved spatial and temporal resolution recent studies have investigated various aspects of grasslands, for example, management [6], [8], soil moisture [7], [9] and classification. Before that, in 1999, Hill et al. [10] conducted a very detailed experiment on grassland biophysical properties using SAR backscatter calculated from multi-frequency (C, L and P band) and multi-polarized (HH, HV and VV) airborne (JPL/NASA airborne imaging system) SAR data. Significant relationships were formulated between the measurement of grass height and the SAR backscatter, demonstrating the potential that might be offered with repeat-pass satellite imagery.

Interferometric coherence is affected by the physical changes of vegetation and ground properties that occur between the acquisition times, a phenomenon known as temporal decorrelation [11]. The coherence is dependent on multiple factors such as: temporal decorrelation, SAR processing, signal to noise ratio, co-registration, volume decorrelation and baseline decorrelation [12]. Studies [13], [14] show that for both SAR interferometry and polarimetric SAR interferometry temporal decorrelation is one major limitation [11] which increases with shorter wavelengths [15].

Right from the day InSAR theory and applications are in place the interferometric analysis (and/or decorrelation) over vegetation (or prime targets covered by vegetation i.e., potential land sliding hot spots) is a challenging task. The main reason behind this inconsistency is predominantly because of volume scattering and temporal decorrelation [15].

In 2014 TerraSAR-X activated a new acquisition mode, staring spotlight (ST) has a longer target illumination time and high spatial resolution (up to 25cm), compared to the high-resolution spotlight (SL) mode (up to 1m). This high spatial resolution is achieved at the cost of spatial coverage, with staring spotlight mode spatial coverage of approximately 4km (width) x 3.7km (length), compared to the SL which covers 10km (width) x 5km (length). TerraSAR-X has an 11-day repeat cycle and is suitable for repeat-pass SAR interferometry analysis. The ST mode is very different from the conventional stripmap mode as the antenna beam keeps staring/focusing at the same ground target for a longer period of time, which

I. Ali is with the Department of Geography, University College Cork and Spatial Analysis Unit, Teagasc, Ireland. In 2015 he was JPL Visiting Student Researcher at Radar Science and Engineering Section at Jet Propulsion Laboratory (JPL/NASA), Pasadena, CA USA. e-mail: iffi.math@gmail.com

B. Barrett is with School of Geographical and Earth Sciences, University of Glasgow, Scotland.

F. Cawkwell is with Department of Geography, University College Cork, Cork, Ireland.

S. Green is with Spatial Analysis Unit, Teagasc Ashtown Dublin, Ireland.

E. Dwyer is with EurOcean - European Centre for Information on Marine Science and Technology

M. Neumann is with Radar Science and Engineering Section at Jet Propulsion Laboratory (JPL/NASA), Pasadena, CA USA.

result in very high spatial resolution.

To the best of our knowledge there is no study reported in the literature on the application of repeat-pass SAR interferometry on managed grassland/pasture to evaluate its potential to monitor biophysical parameters. A recent investigation by Morishita and Hanssen [12] on pasture using repeat-pass multi-frequency SAR interferometry is to analyse and develop a temporal decorrelation model, however no work has been done on the retrieval of grassland biophysical parameters and management practices using spaceborne SAR interferometry. Other investigations on grasslands [16] and crops [17] using X and C-bands are based on Tandem mode SAR acquisitions where the temporal baseline is very short. Zalite et al. [16] shows that even in case of Tandem mode (1 day temporal baseline) the interferometric coherence is highly influence due to temporal decorrelation over vegetated area. Mostly the interferometry analysis on vegetation, especially on crops and grasslands, are undertaken either by using longer wavelengths or with Tandem mode–data acquisition from a sensor constellation.

The results presented here are based on the highest spatial resolution available from a spaceborne SAR sensor. In this experiment we have tested the behaviour of SAR interferometric coherence against the biophysical parameters (height, biomass) of intensively managed pastures and SAR backscatter values. The objective of this study is to investigate the potential and limitations of repeat-pass TSX–ST interferometry to retrieve biophysical parameters of intensively managed grasslands and detection of management practices.

II. Materials and Methods

A. Study site

The study area covers a Teagasc (Irish Agriculture and Food Development Authority) research farm located in the south of Ireland (50° 07′ N, 08° 16′ W). The Teagasc Curtins Research Farm covers an area of 48ha and has a primary focus on sustainable pasture-based dairy systems, grassland and grazing management (see Figure 1). The area has a temperate climate where annual mean temperature ranges from 9.4–10.1 °C, while the annual rainfall varies between 854 and 1208 mm.

B. TSX-ST time series

A time series of TerraSAR-X's newly launched ST mode was acquired from June to November 2014 with a total of 8 acquisitions ([format = acquisition#: ddmmyy] 1: 080614 (wind speed: 2.3 m/s), 2: 190614 (wind speed: 1.4 m/s), 3: 110714, 4: 220714, 5: 020814, 6: 240814, 7: 150914, 8: 091114). All acquisitions have the same specifications (wavelength (λ) = 3.1 cm, incidence angle (θ) = 41.09°, orbit/dir = 147/Asc, polarization = HH, critical baseline = [-15270.66, 15270.66]).

C. In-situ data

Intensive field campaigns were planned on the day of each SAR acquisition in order to collect the grassland height (cm) and biomass (kg DM/ha). For paddock scale biomass (kg DM/ha) estimation, a strip of grass (approximately 1 meter wide and 3.5 meter long) was cut and dried for grassland dry matter (DM) calculation. And for the grass height measurement, an A4 size paper was placed on top of the grass and by using a ruler the height of the paper was taken. For each of the 33 paddocks 12 samples were collected in order to have a mean grass height of the plot. Digital photographs were also taken of each paddock for the purpose of cross validation and analysis.

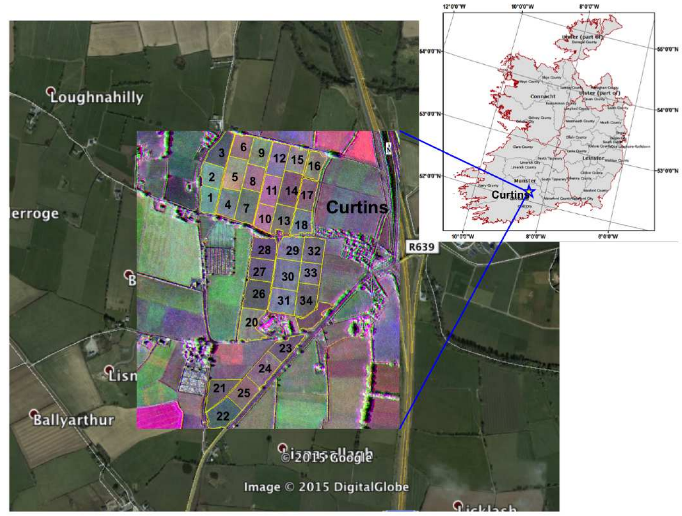

Figure 1: Study site (Curtins, Ireland), A shape file (yellow: overlaid on TerraSAR-X color composite with the Google Earth layer in the background).

III. Methodology

SAR processing for σ^0 [dB]: The TerraSAR-X ST time series data was received as a L1A product in single look complex (SLC) format. After standard preprocessing steps (multi-looking (range looks: 1, azimuth looks: 4), co-registration and multi-temporal filtering) geometric and radiometric calibration was performed to get the backscatter coefficient values of σ^0 (dB), which were geocoded to the Irish Transverse Mercator (ITM) projection.

SAR interferometry processing: For interferometric processing we used the JPL/Caltech SAR interferometric tool ISCE (InSAR Scientific Computing Environment) developed by JPL and Stanford University. The acquisition geometry of the SAR Staring Spotlight mode is different from the Stripmap mode, therefore Doppler rate corrections were implemented as demonstrated by Eineder et al. [18]. These modifications of Doppler rate correction were integrated into the ISCE tool in order to support the TSX–ST mode interferometric processing. Another critical component is the temporal separation between the acquisitions, which is very important for vegetated areas. The volumetric decorrelation has to be taken into account due to the presence of a perpendicular baseline component between the satellites and a vertical distribution of scatterers [19], [20]. Similarly, signal to noise ratio related corrections have already been implemented in the WInSAR (ISCE) toolbox.

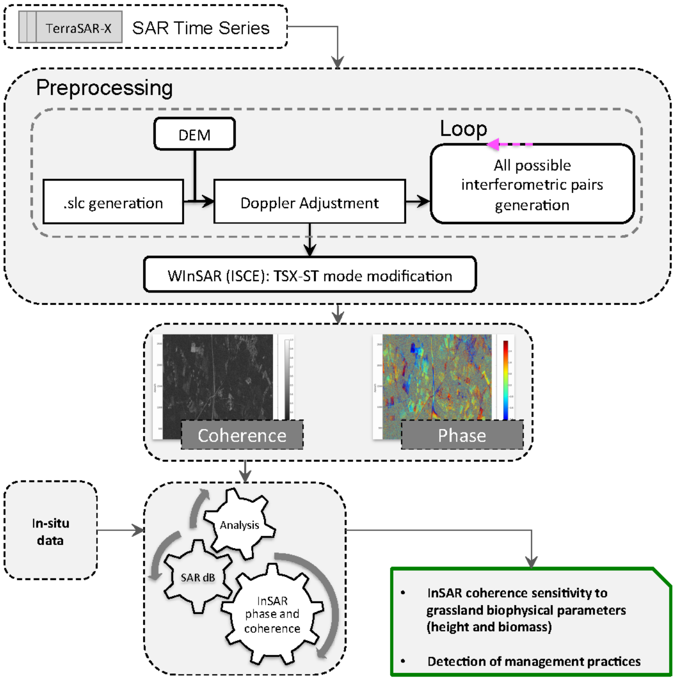

Figure 2: InSAR processing workflow scheme.

All 28 possible interferometric pairs were generated, and the SRTM digital elevation model of 30 meters resolution was used to calculate and remove the topographic phase. For each pair, flattened interferometric coherence and phase were calculated for further analysis.

IV. Results and Discussion

A. *Utility of repeat-pass InSAR time series for investigating grasslands*

Wegmuller and Werner [21] have addressed the issue of temporal decorrelation for spaceborne repeat-pass InSAR over vegetated areas. Studies show that the effect of temporal decorrelation decreases in the case of TanDEM mode–data acquisition from a constellation of SAR sensors e.g., TanDEM-X, ERS-1/2 and COSMO-SkyMed–SAR acquisitions [22], [23], due the very short temporal baseline. The temporal baseline for all 28 pairs of ST data has a range from 11 days to 154 days. Due to the rapid temporal decorrelation over vegetated areas, it was decided to use only the three pairs with the 11-day temporal baseline.

The X-band SAR signals are scattered back to the antenna by the upper canopy component, due to their shorter wavelength (3.1 cm) which cannot fully penetrate through the canopy layer. In case of X-band the signal penetration is mainly depends on the amount of biomass as explained by Hajj et al. [7] that the X-band signal sensitivity to soil moisture decreases when the grassland biomass is more than 1 kg/m^2. In another investigation Brown et al. [24] has reported scattering mechanism for crop parameter retrieval. Due to this sensitivity of the X-band signal to vegetation cover, the decorrelation rate is extremely fast especially during the growing season. In the case of 11-day repeat-pass (110714_220714 and 220714_020814) the correlation between interferometric coherence, the observed parameters (grass height and biomass) and SAR backscatter values is very low as shown in Figure 3. However, the pair 080614_190614 shows a large variation and spread compared to the other two pairs as shown in Figure 3. In this case a high correlation ($R^2 = 0.52$, $p < 0.05$) between InSAR coherence and SAR backscatter values is observed. For the grass height and biomass, correlation values are low ($p > 0.05$) but the spread of the scatter plot is wider in comparison to 110714_220714 and 220714_020814. A detailed investigation is performed in order to understand this behaviour and the variation in the 080614_190614 InSAR pair.

B. *Inter and intra paddock variations*

Due to the shorter wavelength, the X-band signals are very sensitive to small changes in vegetation cover, especially during the growing season when grass grows, and the rate of change of coherent sum of the scatterers in the resolution cell is very high. Figure 4 shows the temporal, as well as the intra- and inter-paddock, variation of the X-band signals for four adjacent grassland paddocks. Grassland paddocks (9 and 15) with short grass height during the first acquisition (080614) (mean height: 2–4 cm) can be distinguished from paddocks 8 and 12 with tall grass (mean height: 25–35 cm). It is evident that in paddocks 9 and 15 the backscatter values in 080614 decreased in the later acquisitions (190614 and 110714) due to the grass growth. This variation is one of the main reasons that led to the high temporal decorrelation over most of the vegetated areas.

Figure 5 (A) shows an example where the highest correlation over grassland area is observed in the first InSAR pair (080614_190614), and complete decorrelation occurs in all other InSAR pairs except for the roads and urban structures. The potential reasons for decorrelation of the other two 11 days InSAR pairs are discussed in the next section. The analysis was originally performed on all pairs, but the results are not shown here, as decorrelated data do not contribute to pasture biophysical parameters retrieval. For this study, we considered the coherent pair 080614_190614 for further analysis in order to retrieve the biophysical parameters.

C. *Detailed analysis of* 080614_190614 *pair*

1) Change in SAR backscatter and its relation to coherent/non-coherent paddocks: Grassland paddocks with short grass height (low biomass) show higher backscatter (dB) because short grass (or paddocks after mowing) have less diffuse scattering compared to the tall grass, especially in the case of the X-band sensors, where signal backscatter mainly comes from the vegetation top canopy layer.

In the case of managed grasslands, the coherent grassland plots follow three types of backscattering patterns:

I High coherence is also observed over the areas where the change in the mean backscatter is more than 2 dB (similar to the findings reported by Wegmuller and Werner [21]). This is due to the presence of short grass height and gradual regrowth (i.e., paddock: 4, 9, 15, 16, 17, 20, 22, 23, 24, 27 and 28, as an example see paddock 16, 17 and

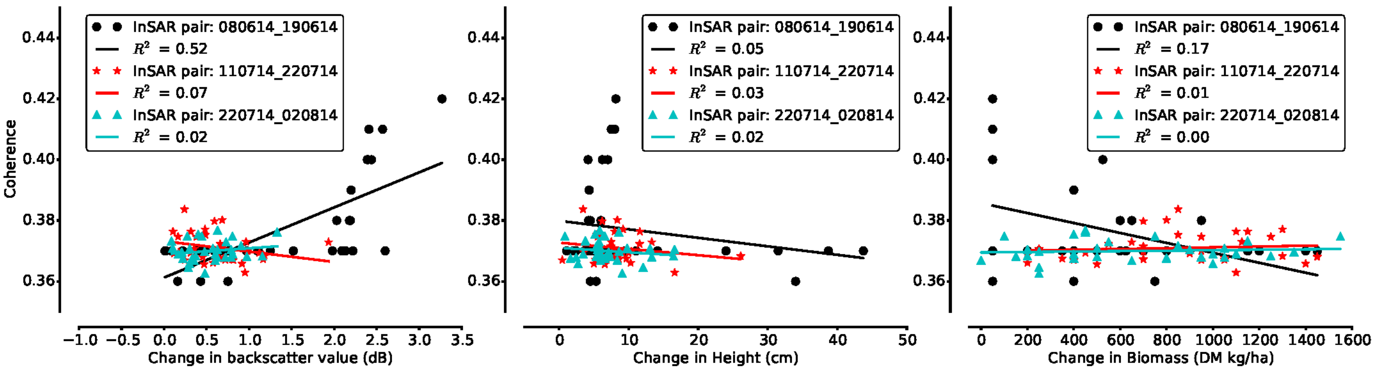

Figure 3: Relationship of calculated coherence with backscatter value, grass height and biomass of three SAR interferometric pairs with 11 days baseline (black = 080614_190614, red = 110714_220714 and cyan = 220714_020814).

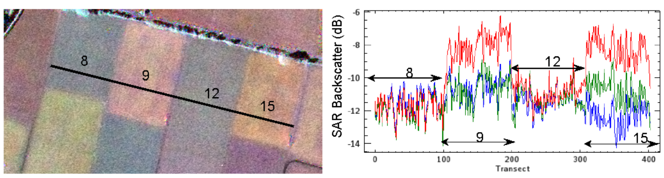

Figure 4: Transect based (black line) backscatter scatter profile of four paddocks (8, 9, 12 and 15) extracted from colour composition of TerraSAR-X staring spotlight mode acquisitions (red=080614, green=190614, blue=110714).

24 in Figure 5 (B) and Figure 5 (C)). In this case ground is complete covered with grass (with only few spots of bare soil) but still the grass is not very tall that it will lay down due to wind.

II Similar to the coherent paddocks (where the change of mean backscatter (dB) is $>$ 2 dB), comparatively less coherent plots (i.e., paddock: 3, 29, 30, 31 and 34) follow the similar pattern where the mean change in backscatter is around 2 dB. Paddock 34 is more coherent than 29 and 30 (as shown in Figure 5 (B)) due to the short grass height in 34 after the intense grazing event.

As we know that value of SAR signal backscatter decrease with the increase of biomass/height as shown in Figure 4 (paddock 15, SAR backscatter value decrease with the gradual grass growth). However, for some paddocks (i.e., 2 and 5) high value of SAR backscatter was observed over tall grass as compared to the short grass (after mowing)–in Figure 5 (C. Plot: 2) image of SAR backscatter is shown. This ambiguity is due to the fact that the grass in the first acquisition (080614) was tall but lying horizontally due to the wind (see Figure 5 (C)). There is however a high backscatter value in the second acquisition (190614) due to the short grass height (after mowing). Similarly in the case of paddock 6, 7 and 8, the difference in backscatter value is due to the gradual grass regrowth (or short grass height in second acquisition as compared to the first).

The different sources (anthropogenic and natural) of decorrelation are thus due to:

i grass growth (i.e., paddock: 6, 7, 8, 11, 12, 13 and 26),
ii grazing (i.e., paddock: 18, 21 and 25), and
iii mowing event (i.e., paddock: 1, 2 and 5)

It can be concluded that from looking at the SAR backscatter only it is not possible to identify the nature of management practices (and/or changes), however by combining both SAR backscatter change and the level of coherence we can identify the type of event that has occurred. For example plot 16 and 17 show a similar change in dB, but 17 is not as coherent as 16 (see Figure 5 (B) and 5 (C)).

We further investigated the reasons as to why the other two 11 day InSAR pairs decorrelated completely except in a few areas. Based on the intensive field validation data it was found that during the month of June most of paddocks are cut for silage, which led to the high coherence due the presence of bare soil and short grass height after cutting. In Figure 5 (A) the InSAR pair 080614_190614 shows that there are many fields outside the study site where high coherence is also achieved due to the silage cut, but in the later acquisitions the InSAR pairs 110714_220714 and 220714_020814 the same fields were decorrelated due to grass growth and high biomass value. For example, in pair 110714_220714 (red inset box in Figure 5 (A)) the upper part is decorrelated due to low backscatter values (or high biomass/grass) while the lower part is coherent due to the high backscatter value (or low biomass/grass), as shown in Figure 5 (D). Similarly in the other pair with 11 days temporal baseline (220714_020814) an example (yellow inset box in Figure 5 (A)) of a coherent patch is shown. These are crop fields where high coherence is due to cutting by the second acquisition and a mean change in SAR backscatter value is more than 2 dB, Figure 5 (E) shows the low backscatter in the first acquisition (220714) and high backscatter in second acquisition (020814).

There are multiple factors that can influence the scattering mechanism of the radar signals and InSAR coherence. And wind speed is one of these factors; high wind speed can displace the scatterers in the resolution cell which will result in complete decorrelation. Tall grass is more susceptible to the wind speed as shown in Figure 5 (C, Plot: 2).

2) Relationship between InSAR coherence and grassland biophysical parameters 080614_190614*:* For the sensitivity analysis of grassland biophysical parameters (height and Biomass) to SAR interferometric coherence, based on the visual assessment the plots under investigation were divided

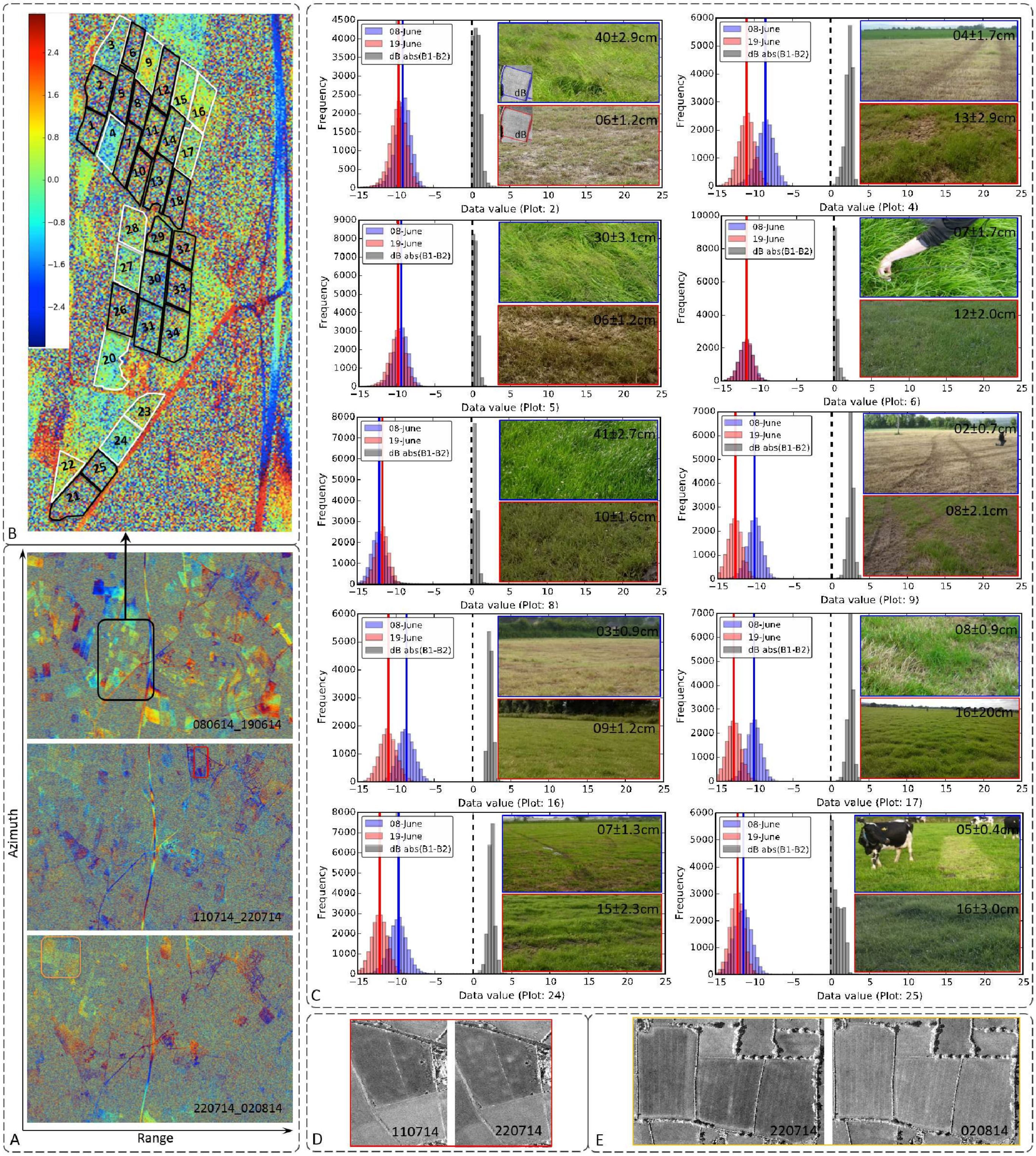

Figure 5: (A): A single baseline interferometric phase (flattened) of three 11 day temporal baseline pairs. (format: ddmmyy$_{master}$_ddmmyy$_{slave}$). (B): InSAR phase (flattened) for pair 080614_190614. Polygons with their number show the plots analysed in this study. Grass plots with white boundaries represents the coherent plots while the plots with black boundaries are non-coherent plots. (C): In each plot (and inset photograph) the blue colour represents the master (080614) and the red colour represents the slave (190614) image. The dark blue lines (080614) and the red lines (190614) represents the mean value of each band, while the dotted black line represents the zero reference. The gray histogram represents the absolute value of the difference between the two acquisitions $abs(080614\_190614)$ for each plot. The mean grass height and standard deviation in cm is also shown for the plots showed as a reference. (D): Example of coherent patch from the pair 110714_220714. (E): Example of coherent patch from the pair 220714_020814.

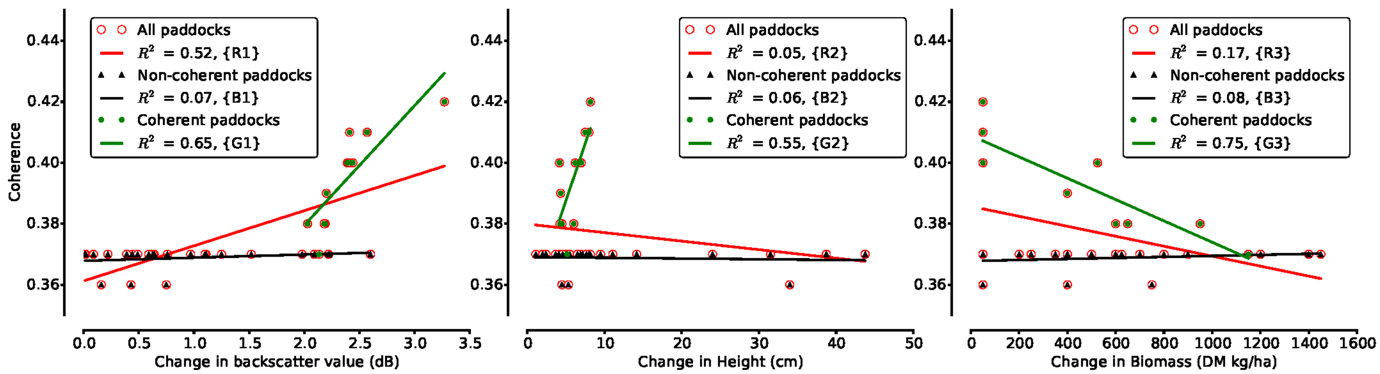

Figure 6: Relationship between calculated coherence with backscatter value (dB) [left], height (cm) [middle] and biomass (kg DM/ha) [right]. Black color represents all the plots, blue points represent the non-coherent plots (plots with black boundaries in Figure 5 (B)) and green points represent the coherent plots (plots with white boundaries in Figure 5 (B)). Color/style of each data point in this figure correspond to the reference regression line.

into three groups: *(i)* all plots shown in Figure 5 (B), *(ii)* non-coherent plots (plots with black boundaries in Figure 5 (B)) and *(iii)* coherent plots (plots with white boundaries in Figure 5 (B)). For each group the relationship of InSAR coherence with the backscatter (dB), grass height (cm) and biomass (DM kg/ha) is discussed.

Coherence versus backscatter: SAR backscatter and interferometric coherence show a good correlation $(R^2 = 0.65,\ p < 0.05)$ for coherent plots $(\{G1\}$: plots with white boundaries) as compared to the non-coherent plots $(\{B1\}$: plots with black boundaries, $(R^2 = 0.07,\ p > 0.05))$ and the combination of both $(\{R1\}$: all plots, $(R^2 = 0.52,\ p < 0.05)$, see Figure 6). The high correlation in case of $\{R1\}$ is due to the inclusion of $\{G1\}$. As discussed in the previous section, it is evident that the absolute change in backscatter values in coherent plots is more than 2 dB, which leads to the high correlation between InSAR coherence and SAR backscatter values for these plots.

Coherence versus height: Figure 6 $\{R2\}$ shows that the coherence and absolute values of change in grass height have a very low correlation for the non-coherent plots (Figure 6 $\{B2\}$). In the case of coherent plots a reverse behaviour is observed $(R^2 = 0.55,\ p < 0.05)$. The reason for this trend is due to the fact that if the change in canopy height is less than 10 cm (or in case of coherent areas/plots) they will either have a constant or increasing trend of height due to the grass growth (see Figure 6 $\{G2\}$). As soon as height starts increasing above the threshold of 10 cm, the coherence will also start decreasing. Similar findings can also be seen in other studies that have been done on grasslands [23] and crops [22].

Coherence versus biomass: Coherent plots (Figure 6 $\{G3\}$) show a strong relationship between the coherence and grassland biomass. High values of coherence occur when there is low biomass (or less percentage canopy cover), and a gradual decrease in coherence is due to the increase of biomass (see Figure 6 $\{R3\}$, Wegmuller and Werner [21] also reported the similar findings). For the coherent paddocks, the relationship between the interferometric coherence and grassland biomass $(R^2 = 0.75,\ p < 0.05, \{G3\})$ is stronger than the relationship with the SAR backscatter $(R^2 = 0.65,\ p < 0.05, \{G1\})$ and grassland height $(R^2 = 0.55,\ p < 0.05, \{G2\})$.

In addition to detecting management practices over intensively managed grassland pastures, the interferometric coherence calculated from high resolution spaceborne data has a great potential to retrieve pasture biomass and height. High coherence over the paddocks cut for silage during the summer season is an important finding especially in terms of calculating carbon budget, as these paddocks show good correlation with the biomass and grass height. The SAR backscatter is an important parameter that can be used in combination with the interferometric coherence in order to determine the type of change that has happened on ground that led to the high or low interferometric coherence.

The backscattered signal results from surface scattering, volume scattering and multiple volume-surface scattering. And it depends on multiple factors i.e., surface roughness, dielectric properties, radar parameters (frequency, polarization, incidence angle) and type of canopy cover [25]. The SAR backscatter is also strongly linked (or responds) to the temporal developments in vegetation, similarly interferometric coherence is very sensitive to the changes in the resolution cell especially for a large temporal baseline over vegetated areas. The effect of temporal decorrelation is minimized in the case of InSAR tandem acquisitions. This investigation was performed on a single farm with very high quality ground truth data and very high resolution spaceborne SAR time series. It is, however, very clear that in order to test the robustness over different vegetation types, this approach must be further investigated on a larger scale including more auxiliary data (e.g., soil moisture, climate variables)

V. Conclusion

In this study we used a very high resolution TerraSAR-X ST time series. Due to the fact that ST acquisition geometry is different from the conventional SAR stripmap mode, geometric and Doppler related adjustments were implemented and later integrated into the ISCE tool. SAR interferometric coherence and phase were calculated for all combinations of baselines. For the detailed analysis we selected three InSAR pairs with an 11-day temporal baseline (080614_190614, 110714_220714 and 220714_020814). For the interferometric pairs 110714_220714 and 220714_020814 the values of correlation between the interferometric coherence and the grassland biophysical parameters were very low, the primary reason for this is due to the de-correlation caused by the grass regrowth after the silage was cut. Initial findings from the June pair show the possibility of change detection due to the grass growth, grazing and mowing events by using InSAR coherence information. However, it is not possible to automatically categorize different paddocks undergoing these changes based only on the SAR backscatter and coherence values, due to the ambiguity caused by tall grass flattened by the wind. Decorrelation over vegetated areas is a very complex and dynamic process which is influenced by many factors, but where there is coherence there is also a good correlation with height and biomass. The lack of coherence suggests that the X-band wavelength is too short, and therefore affected by even minor grass growth, causing decorrelation of the signal. This study concludes that, for X-band SAR interferometry even an 11 day temporal baseline is too long for grassland biophysical parameter retrieval, except for the fields with short grass height or during the cutting season when the grass is cut for silage. After silage cut grass height is short enough that the patches of bare soil are visible which lead to a high coherence over these paddocks. Over the vegetated areas the SAR backscatter behaviour is more consistent and reliable as compare to the interferometric coherence due to the high decorrelation of X-band. Therefore in case of large scale application of InSAR approach to retrieve biophysical parameters it is recommended to collect high quality ground truth information in order to explain the changes in the remote sensing data.

Acknowledgment

We acknowledge the Teagasc Walsh Fellowship Program for funding and German Aerospace Center (DLR) for providing TerraSAR–X data. We thank P. S. Agram (JPL/NASA) for providing and helping with the ISCE toolbox. The research described in this paper was carried out in part at the Jet Propulsion Laboratory (JPL), California Institute of Technology, under a contract with the National Aeronautics and Space Administration (NASA).

References

[1] J. Latham, R. Cumani, I. Rosati, and M. Bloise, "Global land cover SHARE (GLC-SHARE): database beta-release version 1.0-2014," 2014.

[2] J. D. Derner and G. E. Schuman, "Carbon sequestration and rangelands: A synthesis of land management and precipitation effects," *Journal of Soil and Water Conservation*, vol. 62, no. 2, pp. 77–85, Mar. 2007.

[3] I. Ali, F. Cawkwell, E. Dwyer, B. Barrett, and S. Green, "Satellite remote sensing of grasslands: from observation to management—a review," *Journal of Plant Ecology*, 2016.

[4] I. Ali, F. Cawkwell, E. Dwyer, and S. Green, "Modeling managed grassland biomass estimation by using multitemporal remote sensing data - a machine learning approach," *IEEE Journal of Selected Topics in Applied Earth Observations and Remote Sensing*, vol. PP, no. 99, pp. 1–16, 2016.

[5] C. Schuster, T. Schmidt, C. Conrad, B. Kleinschmit, and M. Förster, "Grassland habitat mapping by intra-annual time series analysis - comparison of RapidEye and TerraSAR-x satellite data," *International Journal of Applied Earth Observation and Geoinformation*, vol. 34, pp. 25–34, Feb. 2015.

[6] C. Schuster, I. Ali, P. Lohmann, A. Frick, M. Förster, and B. Kleinschmit, "Towards detecting swath events in TerraSAR-x time series to establish NATURA 2000 grassland habitat swath management as monitoring parameter," *Remote Sensing*, vol. 3, no. 12, pp. 1308–1322, Jun. 2011.

[7] M. E. Hajj, N. Baghdadi, G. Belaud, M. Zribi, B. Cheviron, D. Courault, O. Hagolle, and F. Charron, "Irrigated grassland monitoring using a time series of TerraSAR-x and COSMO-SkyMed x-band SAR data," *Remote Sensing*, vol. 6, no. 10, pp. 10 002–10 032, Oct. 2014.

[8] I. Ali, C. Schuster, M. Zebisch, M. Förster, B. Kleinschmit, and C. Notarnicola, "First results of monitoring nature conservation sites in alpine region by using very high resolution (VHR) x-band SAR data," *IEEE Journal of Selected Topics in Applied Earth Observations and Remote Sensing*, vol. 6, no. 5, pp. 2265–2274, 2013.

[9] I. Ali, F. Greifeneder, J. Stamenkovic, M. Neumann, and C. Notarnicola, "Review of machine learning approaches for biomass and soil moisture retrievals from remote sensing data," *Remote Sensing*, vol. 7, no. 12, p. 15841, 2015.

[10] M. J. Hill, G. E. Donald, and P. J. Vickery, "Relating radar backscatter to biophysical properties of temperate perennial grassland," *Remote Sensing of Environment*, vol. 67, no. 1, pp. 15–31, Jan. 1999.

[11] M. Lavalle, M. Simard, and S. Hensley, "A Temporal Decorrelation Model for Polarimetric Radar Interferometers," *IEEE Transactions on Geoscience and Remote Sensing*, vol. 50, no. 7, pp. 2880–2888, Jul. 2012.

[12] Y. Morishita and R. Hanssen, "Temporal Decorrelation in L-, C-, and X-band Satellite Radar Interferometry for Pasture on Drained Peat Soils," *IEEE Transactions on Geoscience and Remote Sensing*, vol. 53, no. 2, pp. 1096–1104, Feb. 2015.

[13] M. Wei and D. Sandwell, "Decorrelation of L-Band and C-Band Interferometry Over Vegetated Areas in California," *IEEE Transactions on Geoscience and Remote Sensing*, vol. 48, no. 7, pp. 2942–2952, Jul. 2010.

[14] P. A. Rosen, S. Hensley, H. A. Zebker, F. H. Webb, and E. J. Fielding, "Surface deformation and coherence measurements of Kilauea Volcano, Hawaii, from SIR-C radar interferometry," *Journal of Geophysical Research: Planets*, vol. 101, no. E10, pp. 23 109–23 125, Oct. 1996.

[15] H. Zebker and J. Villasenor, "Decorrelation in interferometric radar echoes," *IEEE Transactions on Geoscience and Remote Sensing*, vol. 30, no. 5, pp. 950–959, Sep. 1992.

[16] K. Zalite, O. Antropov, J. Praks, K. Voormansik, and M. Noorma, "Monitoring of agricultural grasslands with time series of x-band repeat-pass interferometric sar," *IEEE Journal of Selected Topics in Applied Earth Observations and Remote Sensing*, vol. PP, no. 99, pp. 1–11, 2015.

[17] M. Santoro, U. Wegmuller, and J. Askne, "Signatures of ERS #x2013;Envisat Interferometric SAR Coherence and Phase of Short Vegetation: An Analysis in the Case of Maize Fields," *IEEE Transactions on Geoscience and Remote Sensing*, vol. 48, no. 4, pp. 1702–1713, Apr. 2010.

[18] M. Eineder, N. Adam, R. Bamler, N. Yague-Martinez, and H. Breit, "Spaceborne Spotlight SAR Interferometry With TerraSAR-X," *IEEE Transactions on Geoscience and Remote Sensing*, vol. 47, no. 5, pp. 1524–1535, May 2009.

[19] P. Rosen, S. Hensley, I. Joughin, F. K.Li, S. Madsen, E. Rodriguez, and R. M. Goldstein, "Synthetic aperture radar interferometry," *Proceedings of the IEEE*, vol. 88, no. 3, pp. 333–382, Mar. 2000.

[20] R. Bamler and P. Hartl, "Synthetic aperture radar interferometry," *Inverse Problems*, vol. 14, no. 4, p. R1, Aug. 1998.

[21] U. Wegmuller and C. Werner, "Retrieval of vegetation parameters with SAR interferometry," *IEEE Transactions on Geoscience and Remote Sensing*, vol. 35, no. 1, pp. 18–24, Jan. 1997.

[22] X. Blaes and P. Defourny, "Retrieving crop parameters based on tandem ERS 1/2 interferometric coherence images," *Remote Sensing of Environment*, vol. 88, no. 4, pp. 374–385, Dec. 2003.

[23] K. Zalite, K. Voormansik, J. Praks, O. Antropov, and M. Noorma, "Towards detecting mowing of agricultural grasslands from multi-temporal COSMO-SkyMed data," in *Geoscience and Remote Sensing Symposium (IGARSS), 2014 IEEE International*, Jul. 2014, pp. 5076–5079.

[24] S. C. M. Brown, S. Quegan, K. Morrison, J. C. Bennett, and G. Cookmartin, "High-resolution measurements of scattering in wheat canopies-implications for crop parameter retrieval," *IEEE Transactions on Geoscience and Remote Sensing*, vol. 41, no. 7, pp. 1602–1610, July 2003.

[25] Y.-Q. Jin and F. Xu, *Polarimetric Scattering and SAR Information Retrieval*, 1st ed. Wiley-IEEE Press, Mar. 2013.